THE JOURNAL OF COMPARATIVE NEUROLOGY 294:325–339 (1990)

VIP- and PHI-Immunoreactivity in Olfactory Centers of the Adult Cat

CLAUDIA SANIDES-KOHLRAUSCH AND PETRA WAHLE
Max-Planck-Institut für Biophysikalische Chemie, Am Faßberg, D-3400 Göttingen, F.R.G.

ABSTRACT

The purpose of the study was to determine the morphology and distribution of vasoactive intestinal polypeptide- and peptide histidine isoleucine-immunoreactive (VIP- and PHI-ir) neurons and innervation patterns in the main and accessory olfactory bulb, anterior olfactory nucleus, and piriform cortex of the adult cat. In these centers, VIP- and PHI-immunoreactive material are present in the same neuronal types, respectively, therefore summarized as VIP/PHI-ir neurons. In the main olfactory bulb, the majority of VIP/PHI-ir neurons are localized in the external plexiform layer. These neurons give rise to two or more locally branching axons. They form boutons on mitral and external tufted cell bodies. According to the morphology and location, we have classified these neurons as *Van Gehuchten* cells. Some VIP/PHI-ir neurons are present in the glomerular layer. They have small somata and give rise to dendrites branching exclusively into glomeruli. We have classified these neurons as *periglomerular cells*. In the granule cell layer, neurons with long apical dendrites and one locally projecting axon are present. In the accessory olfactory bulb, VIP/PHI-ir neurons are localized in the mixed external/mitral/internal plexiform layer. They represent *Van Gehuchten* cells.

In the anterior olfactory nucleus and piriform cortex, VIP/PHI-ir *bipolar basket neurons* are present. They are localized mainly in layers II/III. These neurons are characterized by a bipolar dendritic pattern and by locally projecting axons forming basket terminals on large immunonegative cell somata. Because of their common morphological features, we summarize them as the retrobulbar VIP/PHI-ir interneuron population.

The PHI-ir neurons display the same morphology as the VIP-ir cells. However, they are significantly lower in number with a ratio of VIP-ir to PHI-ir cells about 2:1 in the main and accessory olfactory bulb and in the anterior olfactory nucleus. By contrast, in the piriform cortex the ratio is about 1:1.

Key words: vasoactive intestinal polypeptide, peptide histidine isoleucine, Van Gehuchten cells, bipolar basket cells

Vasoactive intestinal polypeptide (VIP) is present in several regions of the telencephalon of cats, rats, and mice as demonstrated by radioimmunoassay and immunohistochemistry (Lorèn et al., '76; Emson et al., '79; Christophides et al., '83; Obata-Tsuto et al., '83; Beinfeld et al., '84). Peptide histidine isoleucine (PHI), in contrast, has been investigated only by radioimmunoassay (Beinfeld et al., '84; Christophides et al., '84). The studies reported a low content of VIP/PHI in olfactory forebrain centers, suggesting that the peptides are expressed only in a small subset of neurons. The morphology of VIP-ir neurons in olfactory centers has been studied only in the main olfactory bulb of rats and hedgehogs (Gall et al., '86; López-Mascaraque et al., '89) and in the piriform cortex of the cat (Obata-Tsuto et al., '83). A complete study on the morphology of VIP-ir and PHI-ir structures in the rostral olfactory related centers has not yet been undertaken.

It is known that VIP and PHI have molecular similarity, derive from a common precursor gene, and are co-expressed (Christophides et al., '82; Fahrenkrug, '85; Fahrenkrug and Pedersen, '86; Linder et al., '87). Therefore, it could be expected that both peptides are present in neurons of the

Accepted November 1, 1989.

Address reprint requests to Dr. P. Wahle, Max-Planck-Institut für Biophysikalische Chemie, Am Fassberg, D-3400 Göttingen, F.R.G.

same morphology. Indeed, identical neuronal types have been classified in the adult and developing cat neocortex (Wahle and Meyer, '89). The VIP to PHI ratio, however, may vary in different brain regions. The ratio of VIP to PHI is 1:1 in the neocortex, whereas it is 2:1 in the main olfactory bulb (Beinfeld et al., '84). It is unknown whether these differences are reflected by different cell numbers in immunohistochemical material.

In the present study we investigated the morphology of VIP-ir and PHI-ir neurons in the following olfactory centers of the adult cat: main and accessory olfactory bulb, anterior olfactory nucleus, and piriform cortex. In addition, a quantitative analysis of VIP-ir and PHI-ir neuron numbers was carried out in order to determine the VIP to PHI-ir cell ratio. A preliminary report has been published in abstract form (Sanides-Buchholtz and Wahle, '89).

METHODS

Our material consisted of four adult animals (2.5–3.5 kg bodyweight). The animals were deeply anesthetized with sodium pentobarbitone (Nembutal®, 60 mg/kg bodyweight) and perfused through the heart with 0.9% NaCl and 1% sucrose in 0.05 M phosphate buffer pH 7.4 followed by 4% paraformaldehyde, 1% sucrose, and 0.2% picric acid in 0.1 M phosphate buffer, pH 7.4. The brains were removed from the skull. Blocks of the rostral forebrain were soaked overnight in 20% sucrose in 0.1 M phosphate buffer, pH 7.4, for cryoprotection. They were cut into 80 μm thick sections on a freezing microtome in frontal, parasagittal, or horizontal plane. The sections were collected in ice-cold 0.1 M phosphate buffer, pH 7.4, and subsequently processed for immunocytochemistry by using a PAP-method on free floating sections. All washing steps were carried out with 0.05 M Tris-HCl-buffered saline, pH 7.6 (TBS; 50 mM TRIS; 125 mM NaCl), 2% sucrose, and 0.1% BSA. Antibody penetration was enhanced by incubation in 0.2% Triton X-100 in TBS for 1 h. Nonspecific binding sites were blocked by incubation in 3% normal swine serum (NSwS) in TBS for 1 h. Adjacent section pairs were incubated overnight at room temperature in the two following primary antisera, respectively: polyclonal antiserum against vasoactive intestinal polypeptide (VIP), raised in rabbits (dil. 1:700 in NSwS) and polyclonal antiserum against peptide histidine isoleucine (PHI), raised in rabbits (dil. 1:700 in NSwS). In addition, a few triplets of adjacent sections were incubated in VIP-, PHI-, and a mixture of VIP- and PHI-antiserum. The antisera were kindly provided by Prof. J.M. Polak, London (for characterization of antisera see Christophides et al., '83; Bishop et al., '84). Sections were then incubated for 2 h in affinity purified swine-anti-rabbit IgG diluted 1:10, and for another 2 h in PAP-complex (rabbit) diluted 1:50 (secondary antibodies were purchased from DAKO PATTS, Hamburg). The peroxidase reaction product was developed by using 0.03% diaminobenzidine-tetrahydrochloride (Sigma) and 0.001% H_2O_2. The sections were mounted and dried. The reaction product was intensified by treating the slides with 1% OsO_4 in 0.1 M phosphate buffer for 2 min. Thereafter, the sections were dehydrated, cleared, and coverslipped. In controls, staining was totally abolished by adding 100 μg of the peptide (VIP and PHI, porcine, synthetic, Sigma) to 1,000 μl antiserum 30 min prior to incubation, or by substitution of the primary antiserum with affinity purified normal rabbit IgG (DAKO) diluted 1:1,000 in NSwS, or by omitting the primary antiserum.

Series of alternate sections were stained with 0.2% Thionine in order to visualize anatomical structures. The anatomical structures were identified according to the atlas of Berman and Jones (1982). The morphology of VIP-ir and PHI-ir neurons was analyzed with a Leitz Dialux 20 photomicroscope by camera lucida drawings (final magnification ×800). The distribution of VIP-ir and PHI-ir neurons and axon plexuses were documented by camera lucida drawn panels through all layers of the main olfactory bulb, the anterior olfactory nucleus, and the piriform cortex.

In order to determine the number of VIP-ir to PHI-ir neurons, all pairs and triplets of adjacent sections incubated in either VIP- or PHI- or VIP/PHI-mixed antiserum, respectively, were analyzed in the piriform cortex, anterior olfactory nucleus, accessory olfactory bulb, and main olfactory bulb. The latter contained three different cell types which were counted separately. The position of immunoreactive neurons were marked with the aid of an XY-plotter attached to the stage of the microscope. The immunoreactive neurons were counted from the plots. The differences in VIP-ir and PHI-ir neuron numbers per cell type were tested for significance by Wilcoxon test ($P = 0.05$). Neurons of the main olfactory bulb granule cell layer were excluded from significance test, because their total cell number was too low for a statistical analysis.

RESULTS

The immunohistochemical procedure resulted in Golgi-like stained VIP-ir and PHI-ir neurons. This allowed the analysis of dendritic and axonal patterns. The comparison of VIP-ir and PHI-ir stained sections revealed that in the olfactory centers examined VIP-ir and PHI-ir material is present in the same cell types. Therefore, in the morphological description, we summarized the immunoreactive elements as VIP/PHI-ir structures. However, in the main olfactory bulb (MOB), the accessory olfactory bulb (AOB), and the anterior olfactory nucleus (AON), the number of VIP-positive cells exceeded the number of PHI-labeled neurons (Fig. 1; see also Figs. 4a–c, 6a–c, 9a–c), whereas in the piriform cortex (PC) equal numbers were observed (Fig. 1; see also Fig. 11).

In the present paper we use the terminology for the MOB and AOB layers as in our previous study (Sanides-Kohlrausch and Wahle, '90). AON and PC are divided into layer I (molecular layer), layer II (pyramidal layer), and layer III

Abbreviations

AOB	accessory olfactory bulb
EPL	external plexiform layer
FL	fiber layer
GL	glomerular layer
GRL	granule cell layer
IPL	internal plexiform layer
LOT	lateral olfactory tract
ML	mitral cell layer
MOB	main olfactory bulb
AON	anterior olfactory nucleus
AONe	anterior olfactory nucleus; external division
OT	olfactory tubercle
PC	piriform cortex
wm	white matter
I	layer I (molecular layer)
II/III	layer II/III (pyramidal/polymorph layer)

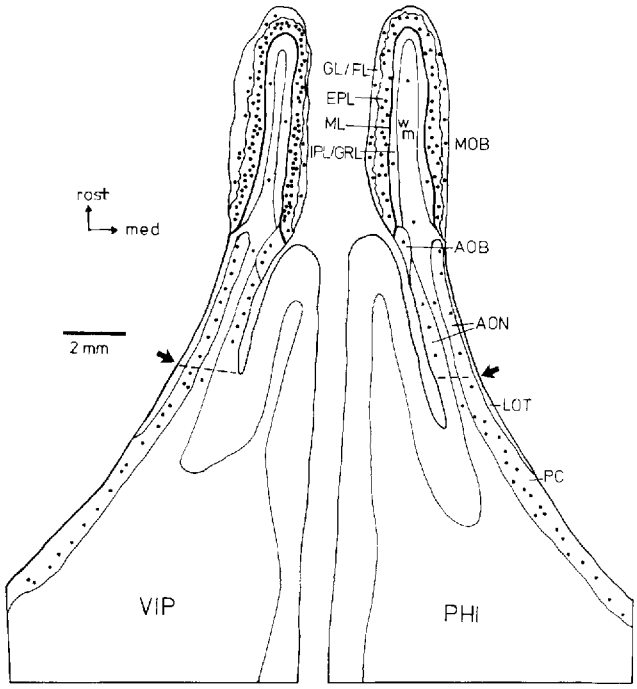

Fig. 1. Distribution of VIP-ir and PHI-ir neurons in cat olfactory centers in schematically drawn sections of the horizontal plane. Position of immunoreactive neurons are indicated by dots. Every dot represents two immunoreactive neurons. Note that in the MOB EPL, the AOB, and the AON, VIP-ir neurons (to the **left**) are much more numerous than PHI-ir neurons (to the **right**). Arrows and dashed lines mark the PC/AON border.

(polymorph layer) according to Price ('73). However, it is difficult to distinguish layers II and III in the VIP/PHI-ir stainings. Therefore we summarized them as layers II/III.

Main olfactory bulb

The distribution of VIP/PHI-ir neurons in the MOB is shown in Figure 1. Immunoreactive somata were observed in the glomerular layer (GL), the external plexiform layer (EPL), the granule cell layer (GRL), and white matter. The overview panel in Figure 2 summarizes the distribution of VIP/PHI-ir somata, fibers, and terminals in more detail (here shown for PHI-immunoreactive material). VIP/PHI-ir terminal puncta were present in the GL, mainly in the glomeruli, and in the EPL, surrounding the VIP/PHI-ir neurons of this layer. A dense fiberplexus was located in the deep aspect of the GRL. Single immunoreactive fibers were also present in the superficial aspect of this layer and in the white matter. The layer of the olfactory nerve fibers was void of immunoreactive processes.

The majority of VIP/PHI-ir neurons were located in the EPL (Figs. 3d–g, 4b,c,g). The neurons had ovoid somata (diameter about 12 μm). They gave rise to two or more thick primary dendrites which remained in the EPL. The processes branched infrequently, followed sinuous or tortuous courses, and bore irregularly arranged slight swellings. The characteristic feature of the EPL neurons were finer, beaded processes which arose from primary dendrites. The finer processes branched very frequently, forming plexuses of a complexity difficult to reconstruct. These plexuses filled the EPL, and occasionally extended into ML, but were not observed to pass into the IPL. The plexuses were very similar to axon terminal fields. Every neuron examined gave rise to at least two of such axon-like terminal plexuses. High-power Nomarsky optics revealed that VIP/PHI-ir boutons were in close contact to large immunonegative somata and proximal processes, most probably representing mitral and tufted cells (Fig. 4h,i). As will be discussed below, we consider these immunoreactive neurons as *Van Gehuchten cells*.

In the GL, two VIP/PHI-ir cell types were observed. The first type (Figs. 3a,b, 4d,e) had small round or ovoid somata (diameter less than 10 μm). The neurons were localized at the surface of glomeruli and gave rise to one primary dendrite invading and ramifying within a glomerulus. The dendritic ramifications of higher order were very fine. Dendrites extending in the glomerular intersticies were not observed. The neurons gave rise to an axon (Fig. 3a,b, arrows). It could be followed only over a very short distance in the glomerular intersticies. In size and distribution these neurons corresponded to *periglomerular cells* as classified by Cajal ('11), Pinching and Powell ('71), and Schneider and Macrides ('78).

The second type was very similar to the *Van Gehuchten cells* of the EPL. It could be distinguished from the *periglomerular cells* by larger somata (diameter about 12 μm). Furthermore, the dendrites extended preferentially into the glomerular intersticies (Figs. 3c, 4f). Axon-like plexuses arose from the dendrites. We had the impression that the plexuses covered the surface of the glomeruli, because they could not be traced into the depth of a glomerulus. We considered these neurons as displaced *Van Gehuchten cells*.

A few VIP/PHI-ir neurons (less than 5% of the VIP/PHI-ir population) were located in the GRL and white matter of the MOB (Fig. 5). Their soma diameter was about 12 μm. The neurons were bipolar (Fig. 5a,d,e) or unitufted (Fig. 5b,c). The dendritic fields were columnar and oriented perpendicularly to the pial surface. Apical dendrites usually branched into elaborate distal tufts with side branches of horizontal course. The tufts generally ended in the IPL. Rarely, single branches invaded the ML or deep EPL. The dendritic profiles were mainly smooth. Occasionally, spines were found at distal dendritic portions. Basal dendrites were shorter (Fig. 5c,d,e) and were oriented perpendicularly or obliquely to the pial surface.

VIP/PHI-ir neurons of the GRL gave rise to an axon which originated from the basal somatic pole (Fig. 5a,b,c,d) or the proximal part of a dendrite (Fig. 5e). The axon initial segments were of variable length. The axons were very thin and regularly beaded. Often, they immediately bifurcated into two collaterals. These formed local plexuses (Fig. 5c,d,e). The longest collaterals observed extended for about 500 μm (Fig. 5f). The axons resembled basket cell axons. However, we could not identify target structures with Nomarsky optics. The collaterals avoided the granule cell clusters.

Accessory olfactory bulb

The cat AOB contained VIP/PHI-ir neurons (Fig. 6b,c). They were localized in the EPL/ML/IPL (see legend to Fig. 6). The neurons had round or ovoid somata (diameter about 12 μm). Primary dendrites were short and thick. They gave rise to several fine, beaded axon-like processes which terminated in the EPL/ML/IPL (Figs. 6d, 7). Their distal portions were found in close proximity to large immunonegative cell bodies, probably mitral cells. VIP/PHI-ir neurons

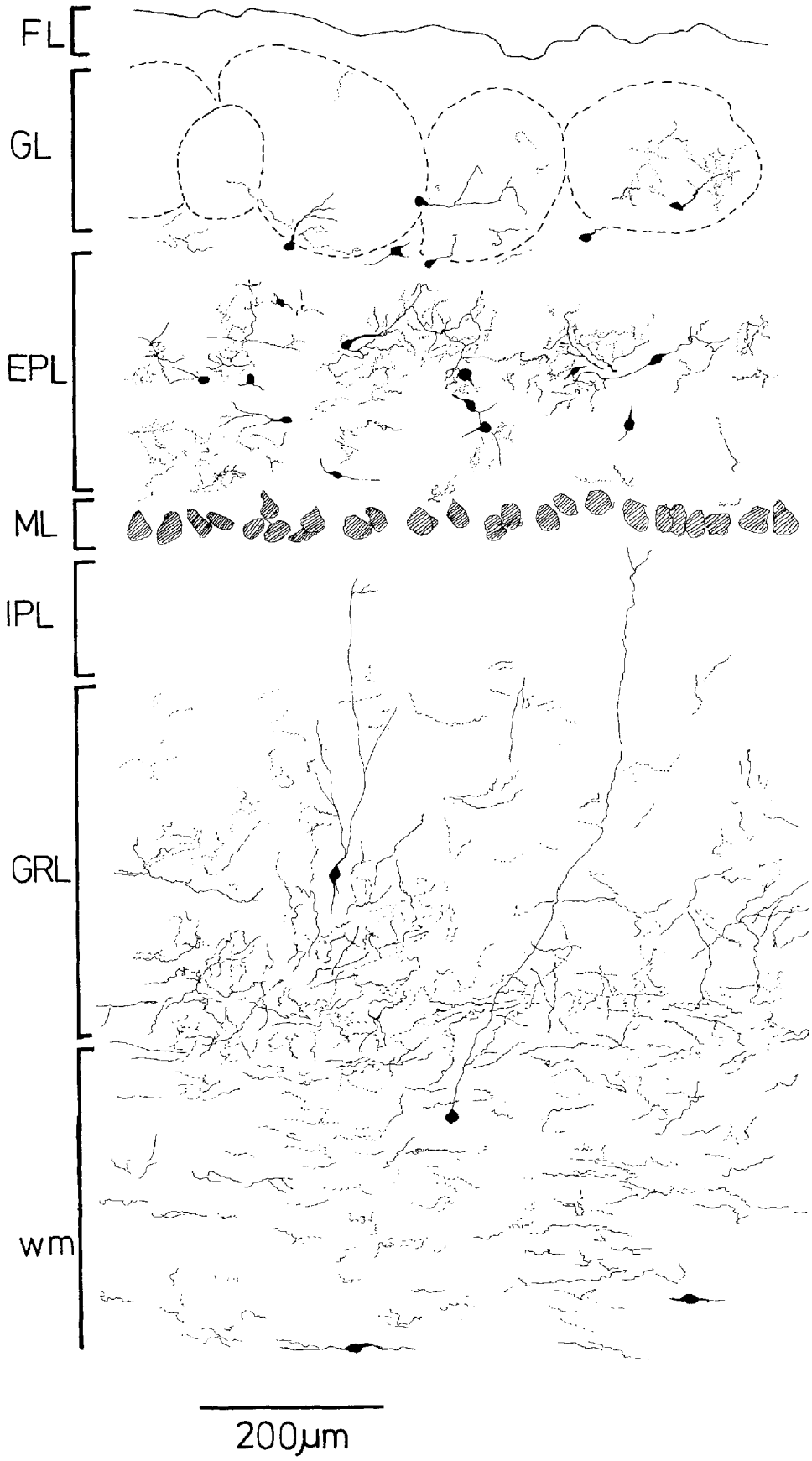

Figure 2

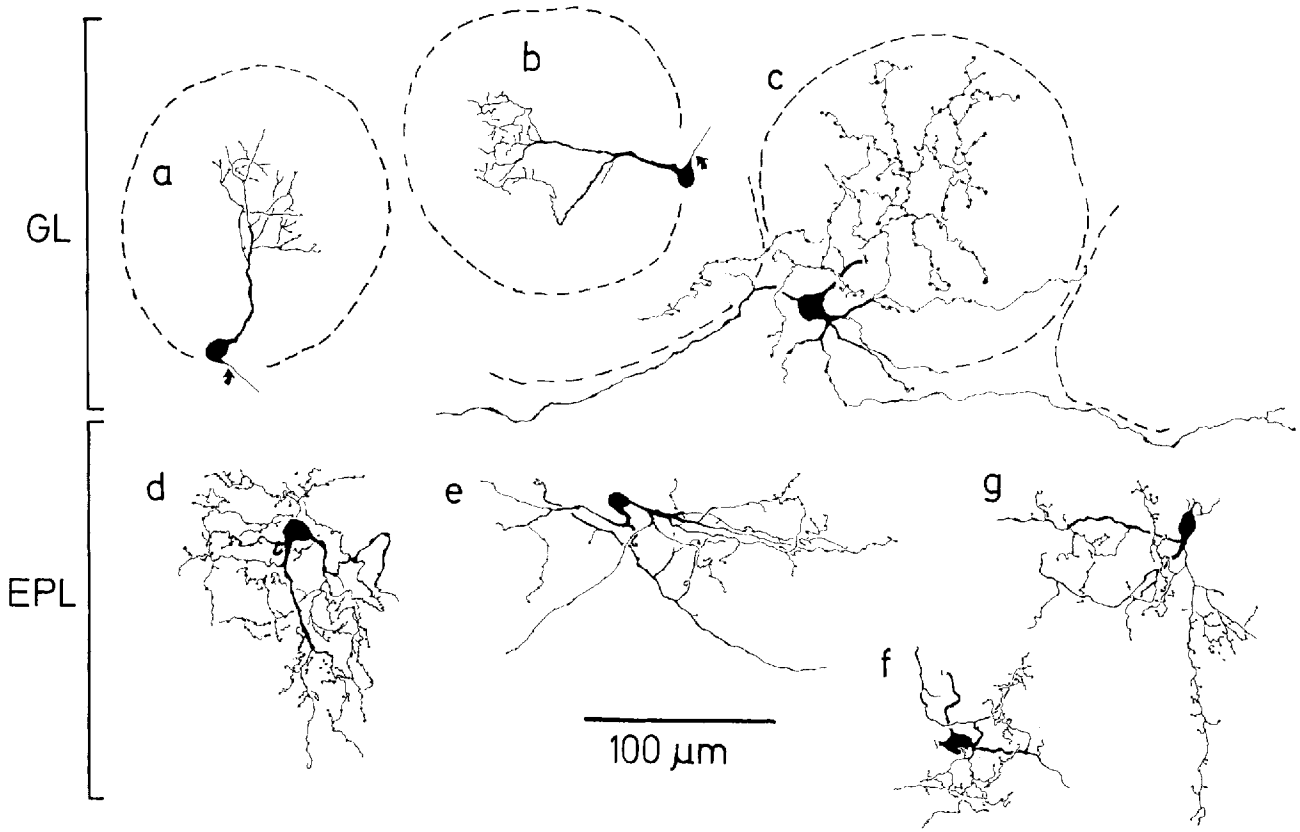

Fig. 3. Camera lucida drawings of GL and EPL VIP/PHI-ir neurons. **a–c** are neurons of the GL; dashed lines symbolize outlines of glomeruli; neurons in a,b are periglomerular cells (axons are indicated by arrows). c is a displaced Van Gehuchten cell (corresponding to Fig. 3f). **d–g:** Van Gehuchten cells. All neurons are drawn from PHI stained material.

of the AOB strikingly resembled the *Van Gehuchten cells* present in the EPL of the MOB.

Anterior olfactory nucleus, piriform cortex

The distribution of VIP/PHI-neurons and axon terminals in the AON is given in the overview drawing of Figure 8a (here drawn from PHI-ir material) and in Figure 9b,c. About 70% of the VIP/PHI-ir somata were located in layers II/III, the rest lay in layer I. The layers II/III were covered with a dense plexus of immunoreactive puncta. The plexus density decreased towards the white matter. This pattern was observed in all subdivisions of the AON. Only in the external division of the AON was the terminal density somewhat higher. This might be due to the densely packed cells in this AON subdivision. The VIP/PHI-ir staining pattern in the PC was very similar to the AON (compare the overview drawings in Fig. 8a,b). The VIP/PHI-ir plexus density abruptly decreased at the transition of the PC to the olfactory tubercle. The cat olfactory tubercle, subdivided into cortical parts and cap regions by Meyer and Wahle ('86), contained very few VIP/PHI-ir neurons in the lateral cortical parts, probably displaced from the adjacent PC. Correspondingly, the plexus density in the cortical parts was low (not shown).

The morphology of the VIP/PHI-ir neurons in the AON and the PC was the same. Neurons had round or ovoid somata (diameter about 12 µm). Most were unitufted (Figs. 9d, 10c,d) or bipolar (Figs. 9e, 10a,b). A few were multipolar (Figs. 9e, 10e). Their large apical dendritic trees were oriented perpendicular to the pial surface. The dendritic tufts fanned out in layer I and might reach the pial surface. The most distal dendritic portions also invaded the lateral olfactory tract (Fig. 8a), where it was prominent superficial to layer I of AON and PC. Dendrites were smooth until they reached the superficial half of layer I. Here, they became more and more varicose and occasionally bore spines (Fig. 9g). Basal dendrites were rarely found.

The VIP/PHI-ir neurons gave rise to an axon. It arose from the basal somatic aspect. After an initial segment of variable length, axons generally bifurcated into two equal collaterals (Figs. 9d, 10). All collaterals were fine and beaded. They formed local plexuses in layers II/III and basket terminals on large immunonegative somata (Fig. 8f), presumably pyramidal cell bodies.

Quantitative analysis

The result of our quantitative analysis is given in Figure 11. The cell numbers of VIP-ir *Van Gehuchten cells* in MOB and AOB, and of VIP-ir AON neurons were always about twice the number of the PHI-ir cells. The difference

Fig. 2. The camera lucida drawing through the MOB layers shows the distribution of PHI-ir structures. Layers are indicated; dashed circles symbolize outlines of glomeruli; hatched cell bodies represent immunonegative mitral cells.

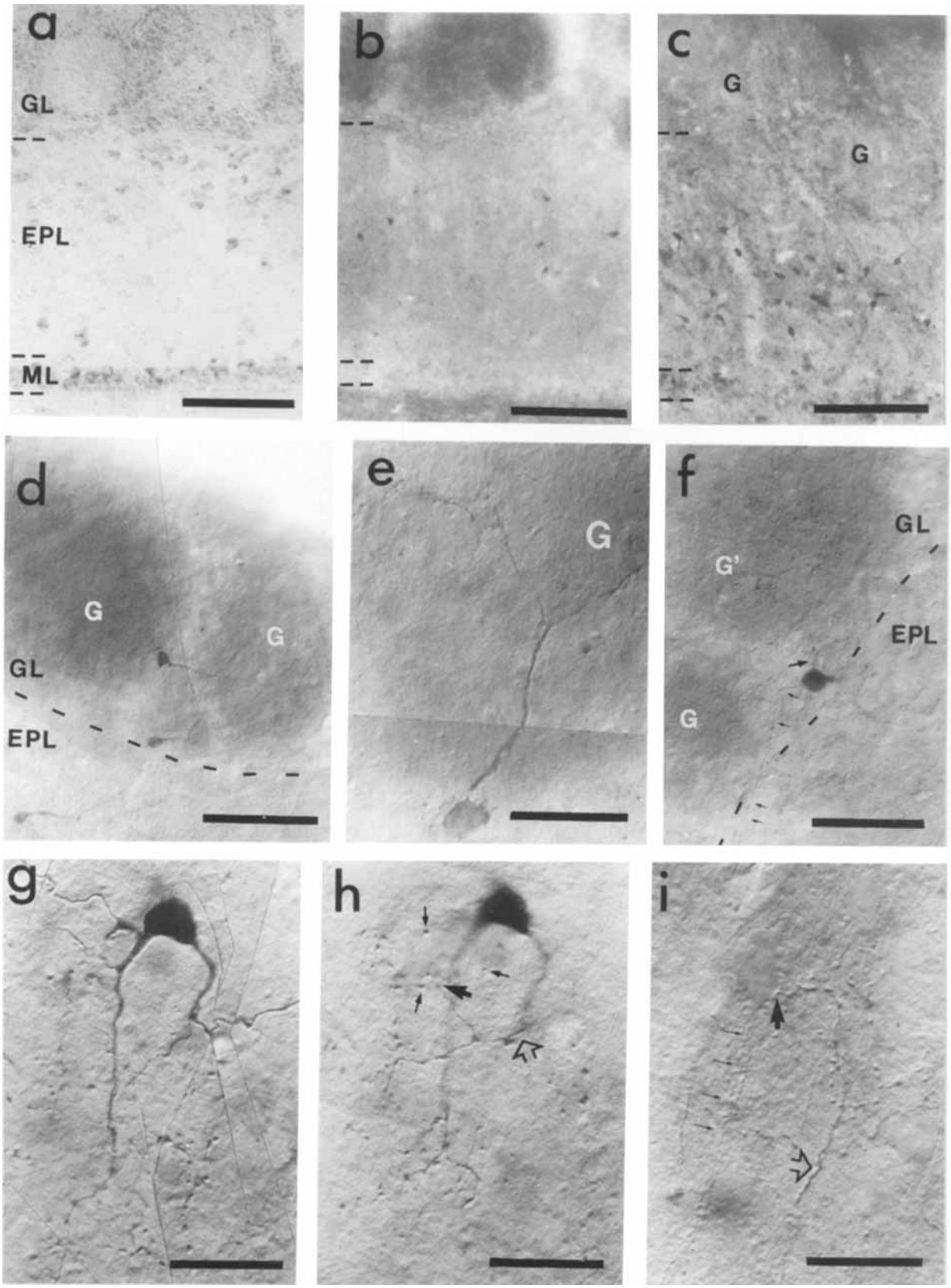

Figure 4

was significant at $P = 0.05$ (Wilcoxon test). In contrast, the *periglomerular cells* of the MOB and the cells of the PC occurred in equal numbers in VIP and in PHI stained material. The slight differences were not significant. Cell numbers counted from material incubated in a mixture of VIP- and PHI-antiserum were not significantly different from the VIP-ir cell numbers.

The total number of VIP-ir or PHI-ir cells per section was dependent upon the size of the section area, whereas the VIP to PHI cell ratio was not dependent upon the size of the section area, on the plane of the section, or on the level of the section in a given plane (compare the sketches with the histograms).

DISCUSSION

Morphology of MOB and AOB neurons

The present study demonstrates VIP/PHI-ir neurons in the cat MOB and AOB, the AON, and the PC, thus confirming data obtained by radioimmunoassay and immunohistochemistry in the rodent brain (Lorèn et al., '76; Emson et al., '79; Gall et al., '86; López-Mascaraque et al., '89) and in cat PC (Obata-Tsuto et al., '83). The PHI content in olfactory structures has been demonstrated, so far, only by radioimmunoassay in the rat PC (Beinfeld et al., '84) and in cat nasal mucosa (Christophides et al., '84).

We have not identified long projecting VIP/PHI-ir fibers in the lateral olfactory tract, the olfactory limb of the anterior commissure, or related to the medial forebrain bundle. Therefore, we conclude that all VIP/PHI-ir neuronal types described in our study represent interneurons. Consequently, we assume that the immunoreactive processes and terminal plexuses, shown in our overview drawings, are produced by axonal or dendritic ramifications of the local VIP/PHI-ir neurons, but do not contain VIP/PHI-ir afferent components. Our results do not confirm the existence of VIP containing afferents from PC or AON to the MOB assumed by Macrides and Davis ('83).

In the MOB, we have identified three different VIP/PHI-ir neuronal types, *periglomerular cells* in the GL, *Van Gehuchten cells* in the GL and EPL, and bipolar neurons with basket axons in the GRL. The VIP/PHI-ir *periglomerular cells* correspond to the original descriptions (Cajal, '11; Pinching and Powell, '71; Schneider and Macrides, '78).

Information about the *Van Gehuchten cell type* is scarce. It is the least characterized cell type of the MOB. Schneider and Macrides ('78) reported the existence of small EPL neurons in Golgi impregnated material, which they termed *Van Gehuchten cells* according to Van Gehuchten and Martin (1891). However, we did not find a specialized interneuron type of the cat EPL mentioned or documented by camera lucida drawings in the original work of Van Gehuchten and Martin (1891). Possibly due to the rare occurrence of *Van Gehuchten cells* in Golgi material it was, so far, hard to document their morphological variety and their common morphological features. Moreover, information on frequency and topography of this cell type is missing. Therefore, *Van Gehuchten cells* do not appear in the bulbar microcircuity models (Shepherd, '72; Holley and McLeod, '77) and their role in the circuity of the bulb is entirely obscure (Nieuwenhuys, '85). More recently, Gall et al. ('86) and López-Mascaraque et al. ('89) identified an EPL cell type in rat and hedgehog material stained with anti-VIP-antisera, which they termed *Van Gehuchten cells* according to Schneider and Macrides ('78), mainly because the type neither corresponds to *periglomerular cells* nor to *superficial short axon cells*. Both studies mentioned an elaborate branching pattern of the processes, but the origin of the fine punctate plexuses was not discussed.

The present study confirms the existence of a VIP/PHI-ir *non-periglomerular* and *non-short axon* cell type in the cat EPL. The type resembles the VIP-ir cells described by Gall et al. ('86) and López-Mascaraque et al. ('89) in distribution, frequency of occurrence, soma size, and conspicuous arborization of the processes. Therefore, we regard this type as *Van Gehuchten cells* of the cat MOB. Our camera lucida reconstructions have revealed that the elaborate arborization results from several axons which arise from the dendrites. Arguments for the axonal nature at the light microscopical level are the fine calibre, the regularly beaded appearance, and the formation of small terminal plexuses. We are aware of the fact that a classification of the fine, beaded *Van Gehuchten cell* processes as axons implies that this cell type gives rise to two or more axons. This, however, does not argue against an axonal character. Neurons with two axons have been described in the visual cortex in Golgi material (Meyer, '82) and in some cholecystokinin-containing cell types (Freund et al., '86; Meyer and Wahle, '88). Freund et al. ('86) confirmed the axonal nature of both axons at the electron microscopical level. Also the "large Golgi cells" in the cerebellum have more than one axon as determined at the light and electron microscopical level (Palay and Chan Palay '74, their Figs. 88, 89). The "Golgi cells" accessory axons are morphologically very similar to the *Van Gehuchten cell* axons.

Schneider and Macrides ('78) discussed the possibility that *Van Gehuchten cells* interact with distal dendrites of granule cells. Our analysis by the aid of Nomarsky optics has revealed that the axonal varicosities are in close contact to mitral cell bodies in the ML and to large cell bodies in the EPL (probably tufted cells). Other boutons are found in the neuropil and may terminate on sub-light microscopic structures, possibly dendrites of mitral and tufted cells or granule

Fig. 4. Photomicrographs of VIP/PHI-ir structures in the MOB GL and EPL. **a–c:** overview panels through the MOB superficial layers: a, Nissl; b, PHI; c, VIP staining; note the low number of PHI-ir neurons. **d:** two PHI-ir periglomerular cells (Nomarsky optics; photomontage); in the EPL a Van Gehuchten cell is present. **e:** PHI-ir periglomerular cell at high magnification (Nomarsky optics; photomontage). **f:** VIP-ir displaced Van Gehuchten cell in the GL (Nomarsky optics); two processes arise from the soma; one process (arrow) forms a large plexus onto the glomerulus (G'); the other process (small arrows) follows the EPL/GL border. **g:** PHI-ir Van Gehuchten cell in the EPL (Nomarsky optics; photomontage). **h:** The same cell in another focus: Neuron gives rise to an axon (open arrow) terminating (small arrows) onto a large immunonegative cell body (nucleus and nucleolus are visible; arrow). **i:** VIP-ir Van Gehuchten cell process (open arrow) in the EPL terminates onto a large immunonegative soma (arrow), of which cell nucleus, nucleolus, and a myelinated axon profile (small arrows) are visible. Nomarsky optics. Glomeruli (G) appear dark in b,d,e,f, due to strong osmium tetroxide treatment. Bar: 250 μm in a–c; 100 μm in d,f; 25 μm in e,g,h,i.

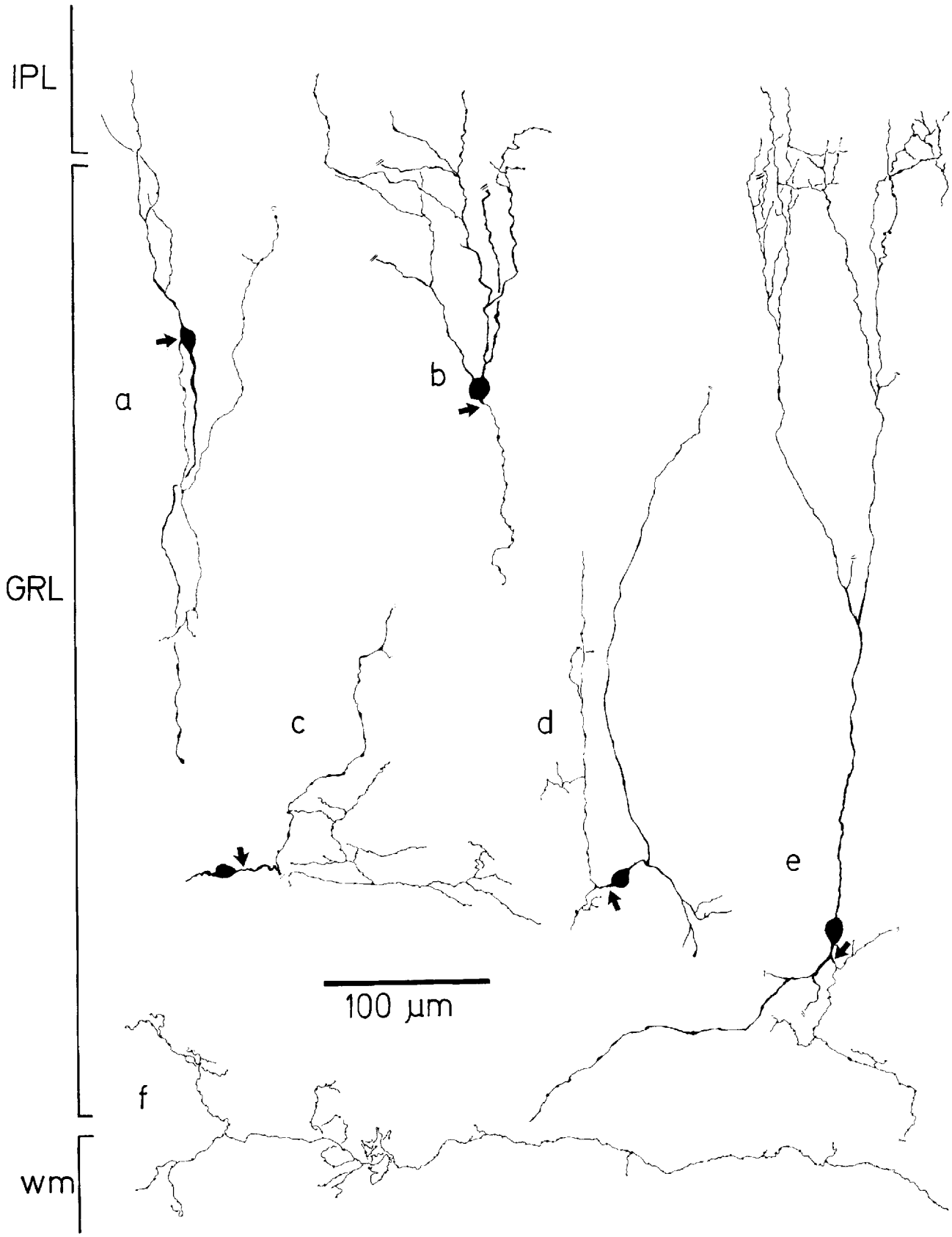

Figure 5

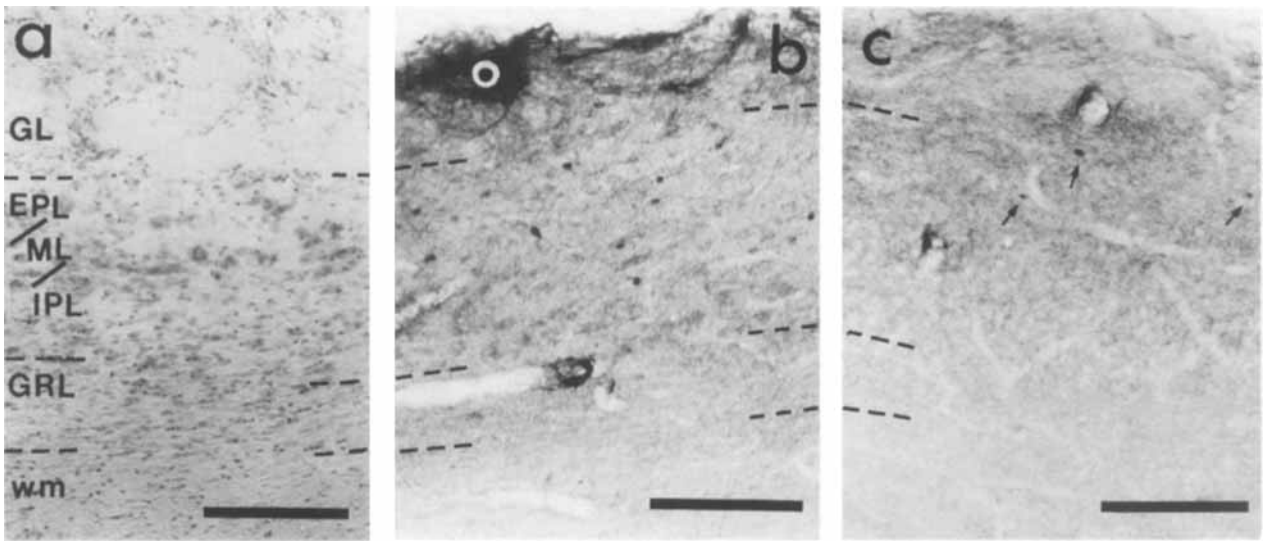

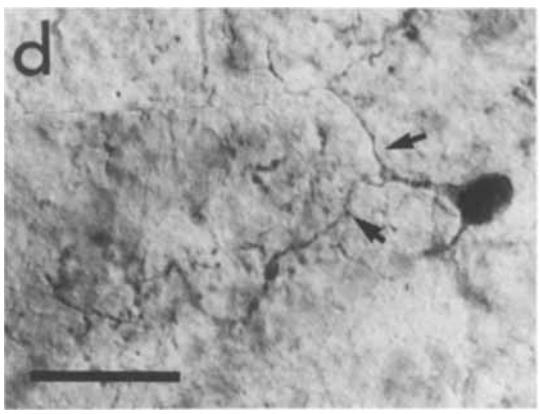

Fig. 6. Photomicrographs of VIP/PHI-ir structures in the AOB. **a–c:** Overview panels through the AOB: a, Nissl; b, VIP; c, PHI stained; layers are indicated: In the cat AOB mitral cells are not aligned in a proper layer, but scatter into the EPL. Often an IPL is not discernible in Nissl stained material. Therefore, we combined EPL, ML, and IPL into one layer EPL/ML/IPL (Sanides-Kohlrausch and Wahle, '90). Note that fewer immunoreactive neurons appear in PHI material (indicated by arrows). **d:** VIP-ir neuron at high magnification; axonal processes are visible, indicated by arrows (photomontage; Nomarsky optics). White circle in b indicates a staining artifact. Bar: 250 μm in a–c; 25 μm in d.

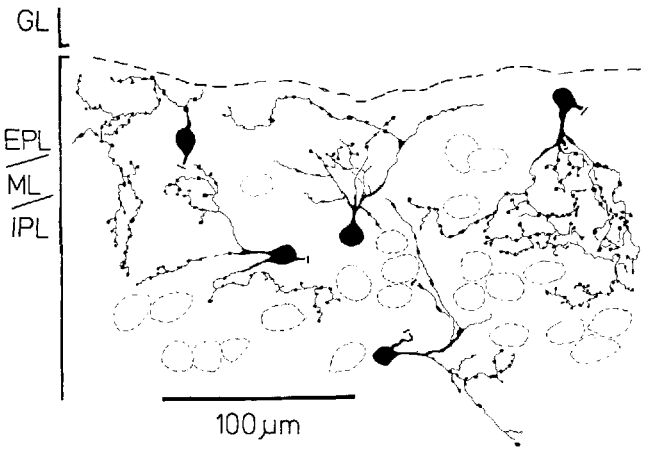

Fig. 7. Camera lucida drawing of VIP/PHI-ir Van Gehuchten cells in the AOB. Dashed line marks the GL/EPL border; dashed ovoid structures symbolize immunonegative mitral cell bodies; neurons are drawn from VIP stained material.

cell dendrites. However, immuno-electron microscopy should confirm the axonal nature of the fine beaded processes of the *Van Gehuchten cells*. Furthermore this would help to identify their targets and would allow to integrate this frequent interneuron type into bulbar microcircuity models.

The VIP/PHI-ir neurons in the GRL have also been documented by Gall et al. ('86) and by López-Mascaraque et al. ('89). They do not resemble Blanes, Golgi, or horizontal cells, documented by Schneider and Macrides ('78) or interneurons shown by López-Mascaraque et al. ('86). Their vertical dendritic pattern vaguely resembles that of Cajal cells. However, those have axons and dendrites ascending into the EPL (Schneider and Macrides, '78). This was not observed in the VIP/PHI-ir neurons.

It is difficult to regard the VIP/PHI-ir GRL neurons as a new bulbar interneuron type. This would imply that their axons terminate on other bulbar neurons. However, we have no evidence for this. Rather, in contrast, fibers accumulate in the deep GRL at the white matter border, and also in the white matter, in this way avoiding the position of Blane, Cajal, Golgi, horizontal, and granule cells. A comparison with VIP/PHI-ir neurons in AON and PC, however, reveals striking similarities in the dendritic arborization and the axonal pattern. On the basis of this morphological similarity, the VIP/PHI-ir neurons of the GRL could be included

Fig. 5. Camera lucida drawings of VIP/PHI-ir neurons of the MOB GRL. Neurons are arranged corresponding to their localization within the GRL. **a,c,d,e** are bipolar cells; **b,** an unitufted neuron. Arrows point to axons. b,c are drawn from PHI; a,d,e from VIP stained material. **f:** PHI-ir basket axon of the deep GRL/wm border.

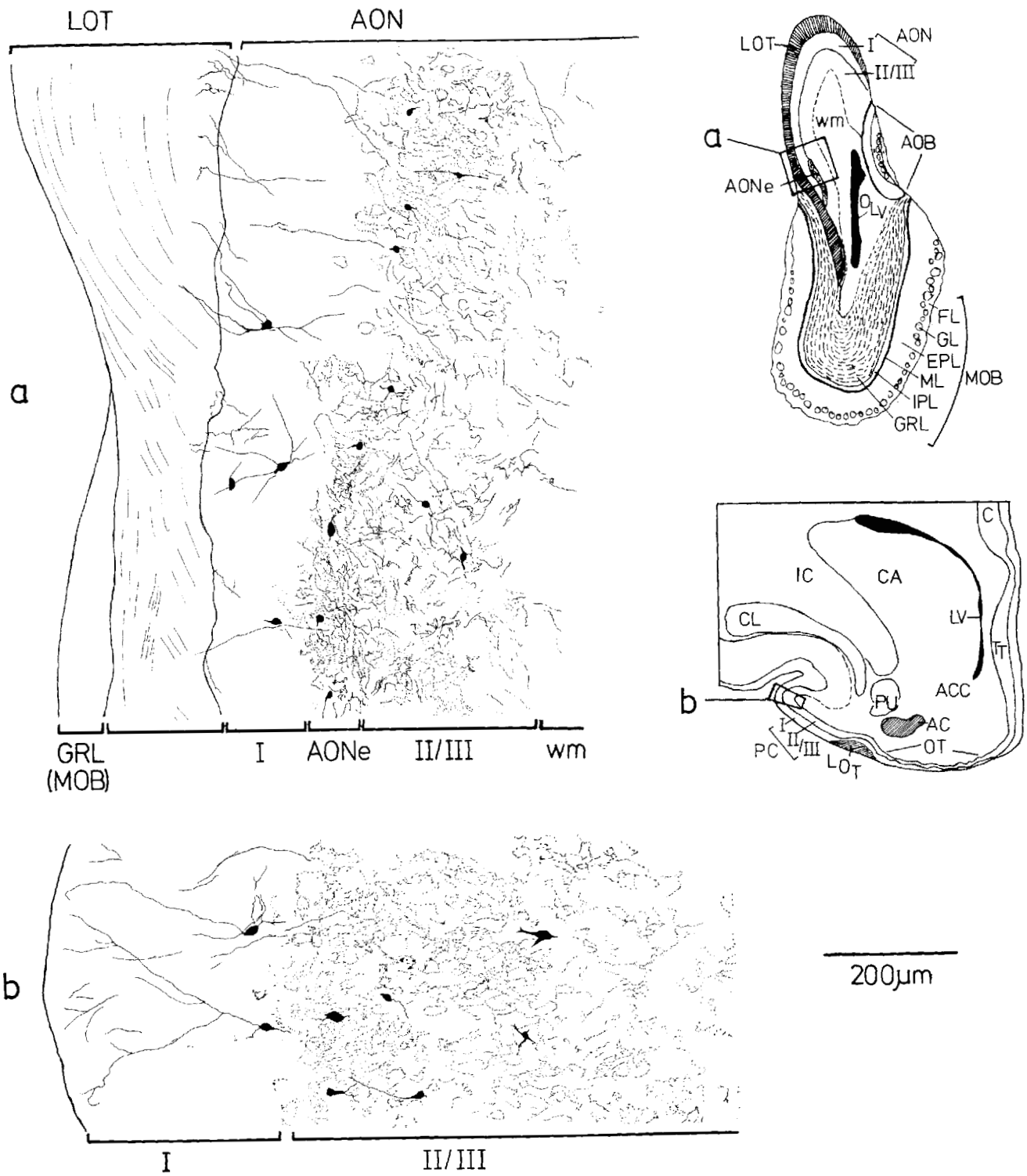

Fig. 8. Camera lucida drawn panels through the layers of the lateral division of the AON and PC show the distribution of PHI-ir structures. **a:** To the **right,** a sketch of a frontal section containing MOB, AOB, AON external division (AONe), and AON lateral division is reproduced. **Boxed area a** is reproduced as panel to the **left** side. Note the higher PHI-ir fiber density in the AONe. The AONe ends about the horizontal midline of the panel. **b:** To the **right,** a sketch of a frontal section through the forebrain containing the PC is reproduced. **Boxed area b** is reproduced as panel to the **left** side. A comparison of this panel with panel a demonstrates the strong resemblance of PHI-ir distribution in PC and AON. AC = anterior commissure; ACC = n. accumbens; CA = caudate nucleus; CL = claustrum; IC = internal capsule; LV = lateral ventricle; OLV = olfactory ventricle; PU = putamen; TT = taenia tecta.

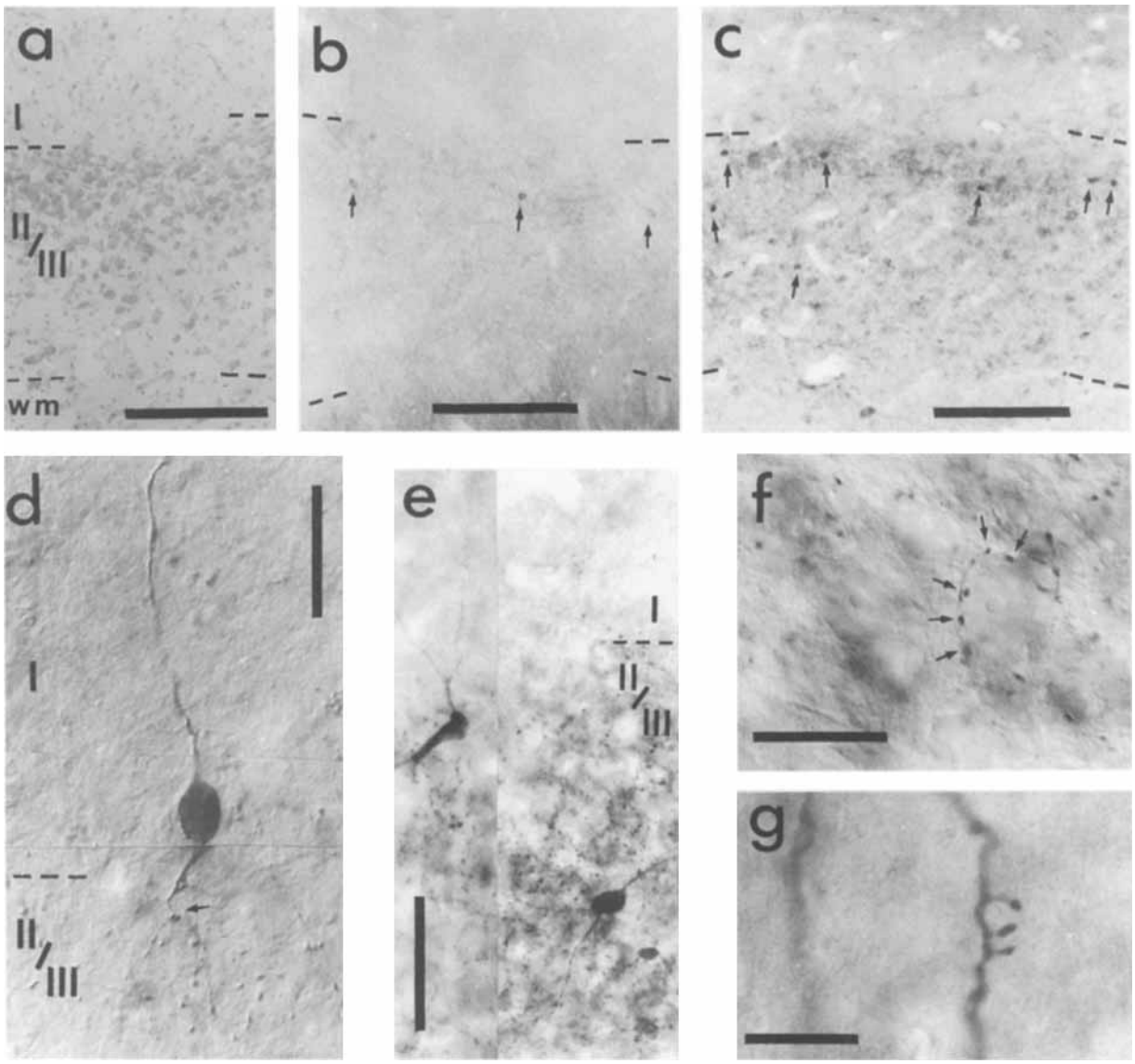

Fig. 9. Photomicrographs of AON and PC VIP/PHI-ir structures. **a–c:** Overview panels through the AON: a, Nissl; b, PHI; c, VIP staining; note that less immunoreactive neurons appear in the PHI stained material (indicated by arrows). **d:** PHI-ir AON neuron; axon bifurcate (arrow) into two collaterals; prominent varicosities are visible (photomontage; Nomarsky optics). **e:** two VIP-ir PC neurons (photomontage); the neuron to the **left** is bitufted; its apical dendrites ascend into layer I. The neuron to the **right** is multipolar and dendrites extend within the layers II/III; note that the layers II/III are densely covered by immunoreactive puncta. **f:** PHI-ir basket terminal onto a large immunonegative soma of which nucleus and nucleolus are visible. The single boutons are indicated by arrows (Nomarsky optics). **g:** spiny distal dendritic portion of a PHI-ir neuron in layer I of the PC. Bar: 250 μm in a–c; 100 μm in e; 25 μm in d,f,g.

into the VIP/PHI-ir population of AON/PC as discussed below.

VIP/PHI-ir neurons in the AOB have not been reported so far. In our material, they resemble in morphology and distribution neither AOB granule cells nor periglomerular cells, which are the only AOB intrinsic neurons with small somata recognized by Golgi, Nissl, and immunohistochemical studies (Cajal, '11; Lohman, '63; Macrides and Davis, '83; Baker, '86; Matsutani et al., '88, '89). Rather, the AOB VIP/PHI-ir neurons resemble VIP/PHI-ir *Van Gehuchten cells* of the MOB. Therefore we conclude that these neurons represent the AOB *Van Gehuchten cell* population. The observation of *Van Gehuchten cells* in the cat AOB indicates that the AOB is composed of more cell types than previously thought.

Morphology of retrobulbar neurons

VIP/PHI-ir neurons of the PC, AON, and MOB GRL display the same morphology. We consider them as one retrobulbar VIP/PHI-ir interneuron population, mainly on the basis of their common axonal pattern, which is the most distinctive criterion for neuronal classification (Jones, '75).

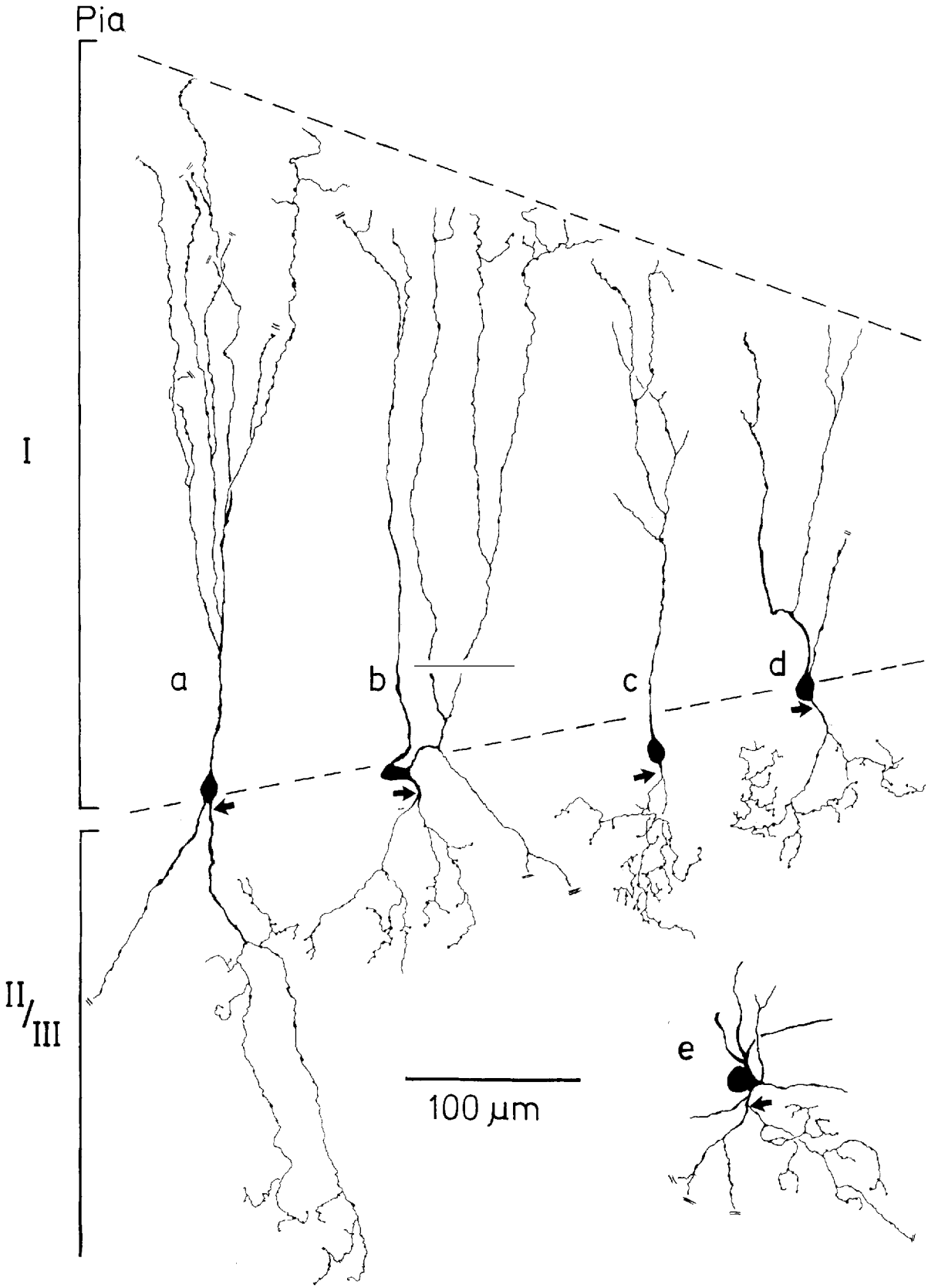

Fig. 10. Camera lucida drawings of AON, PC, and OT VIP/PHI-ir neurons: **a**) PHI-ir bipolar cell from PC; **b**) VIP-ir bipolar cell from a lateral cortical part of the OT; **c,d**) PHI-ir unitufted neurons from AON; **e**) VIP-ir multipolar neuron located in layers II/III. Arrows point to axons.

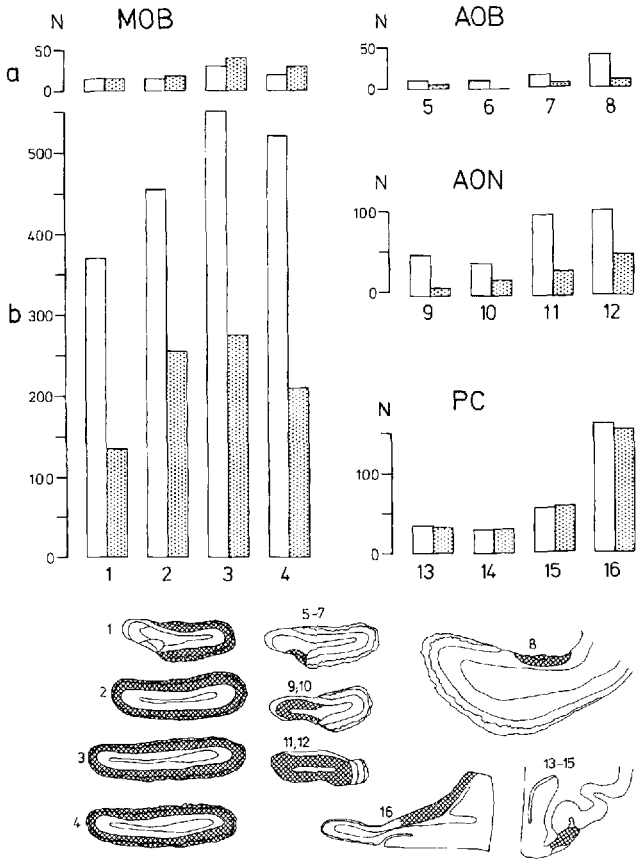

Fig. 11. VIP-ir and PHI-ir neuron numbers in olfactory centers of the cat. Neuron numbers are summarized in histogram form. For every column the open bar represents the VIP-ir cells and the stippled bar the PHI-ir cells counted from adjacent sections. N = number of immunoreactive cells. The columns are numbered from 1 to 16 and the numbers identify the sketches arranged below the histograms. These sketches indicate level, plane, and area (hatched) of the section, from which cells were counted. MOB: Nos. **1–4,** frontal plane. AOB: Nos. **5–7,** frontal plane; No. **8** parasagittal plane. AON: Nos. **9–12,** frontal plane. PC: Nos. **13–15,** frontal plane. No. **16,** horizontal plane. The MOB histogram consist of two parts. Panel a represents numbers of VIP/PHI-ir periglomerular cells; b, VIP/PHI-ir Van Gehuchten cells.

Obata-Tsuto et al. ('83) classified the VIP-ir neurons of the cat PC as bipolar cells solely on the basis of the dendritic pattern. Indeed, the prevailingly bipolar morphology resembles the dendritic pattern of VIP-ir bipolar cells of the rat neocortex. However, both bipolar subtypes of the rat cortex (Peters and Harriman, '88) differ in their axonal morphology from the VIP/PHI-ir bipolar basket cells of the cat PC. Rather, the retrobulbar VIP/PHI-ir neurons correspond to a type, identified in the olfactory cortex of the cat by Cajal ('11; his Fig. 440c), and termed "short axon cell with incomplete baskets" by Pigache ('70). Our results support a classification of the VIP/PHI-ir neurons as basket cells because they have local axons, and boutons in close apposition to immunonegative cell bodies. In this respect the VIP/PHI-ir neurons of the cat AON/PC are similar to the predominant VIP/PHI-ir neuron type of the cat neocortex (Wahle and Meyer, '89). Basket cells are GABAergic interneurons (Hendry et al., '83; Houser et al., '83). The coexistence of VIP and GABA has been demonstrated for neurons in the hippocampus (Kosaka et al., '85) and discussed for neurons in the rat (Meinecke and Peters, '87) and cat neocortex (Wahle and Meyer, '89). The VIP/PHI-ir basket terminal pattern in the layers II/III of the PC strikingly resembles the glutamate-decarboxylase (GAD)-ir terminal pattern in these layers. GAD-ir terminals are also present in layer I (Westenbroek et al. '88; own unpublished observations) which, however, is void of VIP/PHI-ir terminals. Therefore, we suggest that the retrobulbar VIP/PHI-ir neurons of the cat AON/PC are GABAergic, inhibitory in function, and represent a subset of the GABAergic neuron population.

They may function as short-range inhibitory neuronal system. The long apical dendritic tufts distribute in layer I. This is the main input layer containing the bulbar afferents and cortical association fibers (see Haberly and Bower, '89, for a recent review). VIP/PHI-ir neurons may well be exited by afferent fibers and deliver inhibition onto the AON/PC pyramidal neurons. Regarding the high terminal density in the layers II/III and the fact that many terminal boutons are in close apposition to one target cell, the neuron system could be very effective. It could serve as a feed forward inhibitory system (Tseng and Haberly, '88).

The VIP/PHI-ir neurons of the GRL of the MOB which we regard as part of the retrobulbar neuron system may have the same function. Their dendritic tufts end in the IPL. Here, the mitral cell axon collaterals could contact the dendrites. The neurons could then inhibit white matter neurons, possibly cells of the rostral AON division described by Lohman and Mentink ('69).

VIP and PHI expression in the olfactory centers

We have shown that VIP- and PHI-immunoreactivity is present in the same neuronal types. However, our data also reveal different ratios of VIP- and PHI-ir neurons dependent on cell type and/or anatomical center. We either observe equal numbers of VIP- and PHI-ir neurons (e.g., in the PC) or the number of VIP-ir neurons was twice the number of PHI-ir neurons (e.g., in the EPL of the MOB). This did not appear to be due to a lesser sensitivity of the PHI-antiserum. The PHI-ir neurons, as the VIP-ir neurons, are stained in a Golgi-like fashion. Furthermore, different ratios occur horizontal sections, where MOB, AON, and PC are present concurrently. Since our VIP/PHI double stainings did not result in more immunoreactive neurons than the VIP staining alone, we assume that PHI and VIP are co-localized.

Our results confirm biochemical data which demonstrate that the two peptides are co-expressed (Bishop et al., '84; Christophides et al., '82; Fahrenkrug, '85; Fahrenkrug et al., '85; Fahrenkrug and Pedersen, '86; Linder et al., '87). It is, however, difficult to compare our cat immunohistochemical data with radioimmunoassay data obtained from other species. Beinfeld et al. ('84) showed intra- and interspecies differences in concentration and ratio of the two peptides in a given anatomical center. Such differences may explain our finding of another VIP to PHI ratio in the cat PC than reported for the rat PC by Beinfeld et al. ('84).

Since the VIP and PHI messenger RNA concentrations are roughly equal, it was suggested that different VIP to PHI ratios result from differential processing of the precursor peptides in different cell types (Linder et al., '87). In one anatomical center, the MOB, the *Van Gehuchten cells* of the EPL and the *periglomerular cells* in the GL seem to confirm this suggestion: the two neuron types express a VIP

to PHI ratio of 2:1 and 1:1, respectively. On the other hand, classical morphological criteria do not allow us to distinguish between the VIP/PHI-ir neurons of the AON and PC. It is one cell type which could well perform the same function in both centers. However, the AON neurons express VIP to PHI in a 2:1 ratio, whereas in PC neurons a ratio of 1:1 was found. This argues for area-specific processing of the precursor peptides. At present, we do not know which factors influence the differential peptide processing in the different cell types and areas analyzed. Also, the functional role of VIP and PHI in olfactory centers is still unclear. It is known that VIP stimulates cAMP (Magistretti and Schorderet, '84), in this way up-regulating metabolic processes (Magistretti et al., '81). PHI is discussed as an endogenous antagonist at the VIP binding site (Jensen et al., '82). Differential peptide processing could therefore be a mechanism to fine tune rates of energy metabolism in olfactory centers.

ACKNOWLEDGMENTS

We thank Drs. J.M. Polak and J.M. Allen, Hammersmith Hospital, London, for providing us with the excellent anti-VIP and anti-PHI-antiserum. This work was supported by Deutsche Forschungsgemeinschaft Schwerpunkt "Verhaltensontogenie."

LITERATURE CITED

Baker, H. (1986) Species differences in the distribution of substance P and tyrosine hydroxylase immunoreactivity in the olfactory bulb. J. Comp. Neurol. *252*:206–226.

Beinfeld, M.C., D.M. Korchak, B.L. Roth, and T.L. O'Donohue (1984) The distribution and chromatographic characterization of PHI (Peptide histidine isoleucine amide)-27-like peptides in rat and porcine brain. J. Neurosci. *4*:2681–2688.

Bishop, A.E., J.M. Polak, Y. Yiangou, N.D. Christofides, and S.R. Bloom (1984) The distribution of PHI and VIP in porcine gut and their co-localisation to a proportion of intrinsic ganglion cells. Peptides *5*:255–259.

Berman, A.L., and E.G. Jones (1982) The thalamus and basal telencephalon of the cat. A cytoarchitectonic atlas with stereotaxic coordinates. 1st ed. Madison, Wisconsin: The University of Wisconsin.

Cajal, S.R.y. (1911) Histologie du système nerveux de l'homme et des vertebrés II. Paris: Maloine (Reprinted Madrid: Inst. Ramón y Cajal 1955).

Christophides, N.D., Y. Yiangou, N.A. Blank, K. Tatemoto, J.M. Polak, and S.R. Bloom (1982) Are PHI and VIP co-synthetized in the same pro-hormone? Lancet *18*:1398.

Christophides, N.D., G.P. McGregor, P.L. Woodhams, Y. Yiangou, E. Arons, K. Tatemoto, and J.M. Polak (1983) Ontogeny of PHI in the rat brain. Brain Res. *264*:359–361.

Christophides, N.D., J.M. Polak, and S.R. Bloom (1984) Studies on the distribution of PHI in mammals. Peptides *5*:261–266.

Emson, P.C., R.F.T. Gilbert, I. Lorèn, J. Fahrenkrug, F. Sundler, and O.B. Schaffalitzky de Muckadell (1979) Development of vasoactive intestinal polypeptide (VIP) containing neurones in the rat brain. Brain Res. *177*:437–444.

Fahrenkrug, J. (1985) Evidence for common precursors but differential processing of VIP and PHM in VIP-producing tumors. Peptides *6*:357–361.

Fahrenkrug, J., T. Bek, J.M. Lundberg, and T. Hökfelt (1985) VIP and PHI in cat neurons: co-localization but variable tissue content possible due to differential processing. Regul. Pept. *12*:21–34.

Fahrenkrug, J., and J.H. Pedersen (1986) Cosecretion of peptide histidine methionine (PHM) and vasoactive intestinal peptide (VIP) in patients with VIP-producing tumors. Peptides *7*:717–721.

Freund, T.P., Zs. Magloczky, I. Soltesz, and P. Somogyi (1986) Synaptic connections, axonal and dendritic patterns of neurons immunoreactive for cholecystokinin in the visual cortex of the cat. Neuroscience *19*:1133–1159.

Gall, C., K.B. Seroogy, and N. Brecha (1986) Distribution of VIP- and NPY-like immunoreactivities in rat main olfactory bulb. Brain Res. *374*:389–394.

Haberly, L.B., and J.M. Bower (1989) Olfactory cortex: Model circuit for study of associative memory? Trends Neurosci. *12*:258–264.

Hendry, S.H.C., C.R. Houser, E.G. Jones, and J.E. Vaughn (1983) Synaptic organization of immunocytochemically identified GABA neurons in the monkey sensory-motor cortex. J. Neurocytol. *12*:639–660.

Holley, A., and P. McLeod (1977) Transduction et codage des informations olfactive chez les vertebres. J. Physiol. (Paris) *73*:725–828.

Houser, C.R., S.H.C. Hendry, E.G. Jones, and J.E. Vaughn (1983) Morphological diversity of immunocytochemically identified GABA neurons in the monkey sensory-motor cortex. J. Neurocytol. *12*:617–638.

Jensen, R.T., K. Tatemoto, V. Mutt, G. Lemp, and J. Gardner (1982) Actions of a newly isolated intestinal polypeptide, PHI, on pancreatic acini. Am. J. Physiol. *241*:498–502.

Jones, E.G. (1975) Varieties and distribution of non-pyramidal cells in the somatic sensory cortex of the squirrel monkey. J. Comp. Neurol. *243*:205–268.

Kosaka, T., K. Kosaka, K. Tateishi, Y. Hamaoka, N. Yanaihara, J.-Y. Wu, and K. Hama (1985) GABAergic neurons containing CCK-8-like and/or VIP-like immunoreactivities in the rat hippocampus and dentate gyrus. J. Comp. Neurol. *239*:420–430.

Linder, S., T. Barkhem, A. Norberg, H. Persson, M. Schalling, T. Hökfelt, and G. Magnusson (1987) Structure and expression of the gene encoding the vasoactive intestinal peptid precursor. Proc. Natl. Acad. Sci. USA *84*:605–609.

Lohman, A.H.M. (1963) The anterior olfactory lobe of the guinea pig. A descriptive and experimental study. Acta Anat. (Basel) *53(Suppl. 49)*:1–109.

Lohman, A.H.M., and G.M. Mentink (1969) The lateral olfactory tract, the anterior commissure, and the cells of the olfactory bulb. Brain Res. *12*:396–413.

López-Mascaraque, L., J.A. de Charlos, and F. Valverde (1986) Structure of the olfactory bulb of the hedgehog (*Erinaceus europaeus*): Description of cell types in the granular layer. J. Comp. Neurol. *253*:135–152.

López-Mascaraque, L., R.M. Villalba, and J.A. de Charlos (1989) Vasoactive intestinal polypeptide-immunoreactive neurons in the main olfactory bulb of the hedgehog (*Erinaceus europaeus*). Neurosci. Lett. *98*:19–24.

Lorèn, I., P.C. Emson, J. Fahrenkrug, A. Björklund, J. Alumets, R. Hakanson, and F. Sundler (1976) Distribution of vasoactive intestinal polypeptide in the rat and mouse brain. Neuroscience *4*:1953–1976.

Macrides, F., and B.J. Davis (1983) The olfactory bulb. In P.C. Emson (ed): Chemical Neuroanatomy. New York: Raven. pp. 391–426.

Magistretti, P.J., J.H. Morrison, W.J. Shoemaker, V. Sapin, and F.E. Bloom (1981) Vasoactive intestinal polypeptide induces glycogenolysis in mouse cortical slices: A possible regulatory mechanism for the local control of energy metabolism. Proc. Natl. Acad. Sci. USA. *78*:6535–6539.

Magistretti, P.J., and M. Schorderet (1984) VIP and noradrenaline act synergistically to increase cyclic AMP in cerebral cortex. Nature *308*:280–282.

Matsutani, S., E. Senba, and M. Tohyama (1988) Neuropeptide- and neurotransmitter-related immunoreactivities in the developing rat olfactory bulb. J. Comp. Neurol. *272*:331–342.

Matsutani, S., E. Senba, and M. Tohyama (1989) Distribution of neuropeptidelike immunoreactivities in the guinea pig olfactory bulb. J. Comp. Neurol. *280*:577–586.

Meinecke, D., and A. Peters (1987) GABA immunoreactive neurons in rat visual cortex. J. Comp. Neurol. *261*:388–404.

Meyer, G. (1982) Short-axon neurons with two axon-like processes in the visual cortex of the cat. A Golgi study. Brain Res. *232*:455–459.

Meyer, G., and P. Wahle (1986) The olfactory tubercle of the cat I. Morphological components. Exp. Brain Res. *62*:515–527.

Meyer, G., and P. Wahle (1988) Early postnatal development of cholecystokinin-immunoreactive structures in the visual cortex of the cat. J. Comp. Neurol. *276*:360–386.

Nieuwenhuys, R. (1985) Chemoarchitecture of the brain. Berlin, Heidelberg, New York, Tokyo: Springer.

Obata-Tsuto, H.L., H. Okamura, T. Tsuto, H. Terubayashi, K. Fukui, N. Yanaihara, and Y. Ibata (1983) Distribution of VIP-like immunoreactive neurons in the cat central nervous system. Brain Res. Bull. *10*:653–660.

Palay, S., and V. Chan Palay (1974) Cerebellar Cortex. Cytology and Organization, 1st edn. Berlin, Heidelberg, New York: Springer.

Peters, A., and K.M. Harriman (1988) Enigmatic bipolar cell of rat visual cortex. J. Comp. Neurol. *267*:409–432.

Pigache, R.M. (1970) The anatomy of "palaeocortex." A critical review. Ergebn. Anat. Entwickl.-Gesch. *43*:1–62.

Pinching, A.J., and T.P.S. Powell (1971) The neuron types of the glomerular layer of the olfactory bulb. J. Cell Sci. *9*:305–345.

Price, J. (1973) An autoradiographic study of complementary laminar patterns of termination of afferent fibers to the olfactory cortex. J. Comp. Neurol. *150*:87–108.

Sanides-Buchholtz, C., and P. Wahle (1989) Morphology and distribution of vasointestinal polypeptide- and peptide-histidine-isoleucine immunoreactive (VIP- and PHI-ir) neurons in olfactory structures of the adult cat. In N. Elsner and W. Singer (eds): Dynamics and Plasticity in Neuronal Systems. Proceedings of the 17th Göttingen Neurobiology Conference. Stuttgart, New York: Thieme. No. 253 (meeting abstract).

Sanides-Kohlrausch, C., and P. Wahle (1990) Morphology of neuropeptide Y-immunoreactive neurons in the cat olfactory bulb and olfactory peduncle: Postnatal development and species comparison. J. Comp. Neurol. in press.

Schneider, S.P., and F. Macrides (1978) Laminar distributions of interneurons in the main olfactory bulb of the adult hamster. Brain Res. Bull. *3*:73–82.

Shepherd, G.M. (1972) Synaptic organization of the mammalian olfactory bulb. Physiol. Rev. *52*:864–917.

Tseng, G.-F., and L.B. Haberly (1988) Characterization of synaptically mediated fast and slow inhibitory processes in piriform cortex in an in vitro slice preparation. J. Neurophysiol. *59*:1352–1376.

Van Gehuchten, A., and I. Martin (1891) Le bulbe olfactif chez quelques mammiferes. La Cellule *5*:205–237.

Wahle, P., and G. Meyer (1989) Early postnatal development of vasoactive intestinal polypeptide- and peptide histidine isoleucine-immunoreactive structures in the cat visual cortex. J. Comp. Neurol. *282*:215–248.

Westenbroek, R.E., L.E. Westrum, A.E. Hendrickson, and J.-Y. Wu (1988) Ultrastructural localization of immunoreactivity in the developing piriform cortex, J. Comp. Neurol. *274*:319–333.